Springer

KSME

Journal of Mechanical Science and Technology 24 (3) (2010) 811~822
www.springerlink.com/content/1738-494x
DOI 10.1007/s12206-009-1211-9

Bearing fault detection and diagnosis based on order tracking and Teager-Huang transform †

Hui Li[1,*], Yuping Zhang[1] and Haiqi Zheng[2]

[1]*Department of Electromechanical Engineering, Shijiazhuang Institute of Railway Technology, Shijiazhuang, 050041, P.R. China*
[2]*First Department, Shijiazhuang Mechanical Engineering College, Shijiazhuang, 050003, P.R. China*

(Manuscript Received July 29, 2009; Revised August 27, 2009; Accepted September 11, 2009)

Abstract

The vibration signal of the run-up or run-down process is more complex than that of the stationary process. A novel approach to fault diagnosis of roller bearing under run-up condition based on order tracking and Teager-Huang transform (THT) is presented. This method is based on order tracking, empirical mode decomposition (EMD) and Teager Kaiser energy operator (TKEO) technique. The non-stationary vibration signals are transformed from the time domain transient signal to angle domain stationary one using order tracking. EMD can adaptively decompose the vibration signal into a series of zero mean amplitude modulation-frequency modulation (AM-FM) intrinsic mode functions (IMFs). TKEO can track the instantaneous amplitude and instantaneous frequency of the AM-FM component at any instant. Experimental examples are conducted to evaluate the effectiveness of the proposed approach. The experimental results provide strong evidence that the performance of the Teager-Huang transform approach is better to that of the Hilbert-Huang transform approach for bearing fault detection and diagnosis. The Teager-Huang transform has better resolution than that of Hilbert-Huang transform. Teager-Huang transform can effectively diagnose the faults of the bearing, thus providing a viable processing tool for gearbox defect monitoring.

Keywords: Order spectrum; Bearing; Fault diagnosis; Order tracking; Empirical mode decomposition; Hilbert-Huang transform; Teager-Huang transform; Signal processing; Time-frequency analysis

1. Introduction

Fault detection and diagnosis in rolling bearing have been the subject of intensive research. Vibration signal analysis has been widely used in the fault detection of rotation machinery. Many methods based on vibration signal analysis have been developed. These methods include power spectrum estimation, fast Fourier transform (FFT), cepstrum analysis and envelope spectrum analysis, which have been proved to be effective in bearing fault detection. However these methods are based on the assumption of stationary and linear vibration signal. Therefore, new techniques are needed to analyze vibration for fault detection and diagnosis in roller bearing. Bearing faults by their nature are time localized transient events. To deal with non-stationary and non-linearity signals, time-frequency analysis techniques such as the short time fourier transform (STFT) [1], wavelet transform (WT) [2-6], Wigner-Ville distribution (WVD) [7-10] and Hilbert-Huang transform (HHT) [11, 12] are widely used. However when the analyzed vibration signal is composed of many spectral components and with large changes of the machine speed such as run-up or run-down process, they become very difficult to analyze. If the machine operates under varying speed or load, its dynamic and vibration become non-stationary. Fixed time sampling cannot cope with the varying rotational frequency of the machine, resulting in increasing leakage error and spectral smearing. Therefore, most of the conventional methods for signal processing become inappropriate when monitoring the vibrations of varying speed machinery [13, 14]. The reason why we stress the run-up or run-down process is that non-stationary vibrations signals from varying speed machinery may include more abundant information about its condition. Some phenomena, which are usually not obvious at constant speed operation, may become more apparent under varying speed conditions. Therefore, the behavior characteristics of the run-up or run-down process have a distinct diagnostic value, and the fault diagnosis of run-up or run-down process has owed its distinct standing in the fault diagnosis of rotating machinery. In the last decade vibration analysis and condition monitoring techniques for varying speed machinery have attracted the attention of scientists and engineers. Some progresses have been made in the theoretical analysis, the signal processing

† This paper was recommended for publication in revised form by Associate Editor Hong Hee Yoo

*Corresponding author. Tel.: +86 311 8862 1089, Fax.: +86 311 8862 1073
E-mail address: Huili68@163.com

methodology, measurements and practical applications of varying speed machinery monitoring. Lopatinskaia et al. [13, 14] presented the application of recursive filtering and angle domain analysis to non-stationary vibration analysis. The approach is implemented and validated through computer simulation and experiments. Meltzer [15, 16] dealt with the recognition of faults in gear tooth during non-stationary start-up and run-down of planetary gear drives using the time-frequency approach. Wu et al. [17] presented the application of adaptive order tracking fault diagnosis technique based on recursive Kalman filtering algorithm to gear-set defect diagnosis and engine turbocharger wheel blades damaged under various conditions. Li et al. [18] presented the hidden Markov model-based fault diagnosis method in speed-up and speed-down process for rotating machinery.

Recently, order tracking has been become one of the important methods for fault diagnosis in rotating machinery. Potter [19] as well as Potter and Gribler [20] presented the computed order tracking process in which the vibration and speed data is sampled at a constant sampling rate. Fyfe and Munck [21] investigated the factors, which have an effect on computed order tracking. It is indicated that the method is extremely sensitive to the timing accuracy of the key-phasor pulses representing the shaft speed. Higher order interpolation functions were successfully utilized to estimate the rotational speed between key-phasor pulses in order to improve the accuracy of the order tracking process. Bossley et al. [22] evaluated various interpolation algorithms such as linear interpolation, B-spline interpolation, Lagrange interpolation and Fourier series interpolation. A hybrid computed order-tracking approach was proposed to overcome the key-phasor arrival time sensitivity problem of conventional computed order tracking. Vibration signals produced from rotating machinery are speed dependent and hence orders as opposed to absolute frequencies are preferred as the frequency base. Orders represent the number of cycles per revolution and are thus ideal for representing speed-dependent vibrations. Therefore, order tracking normally exploits a vibration or a noise signal supplemented with the information of shaft speed for fault diagnosis of rotating machinery. The order spectrum gives the amplitude of signal as a function of harmonic order and shaft speed in rotating machinery [22].

In recent years, the Hilbert-Huang transform (HHT) has been applied to identification of damage time instant and location in geophysics [23], image processing [24], structural testing [25, fault diagnosis [26], nuclear physics [27] and so on. These applications have further demonstrated the effectiveness of HHT in transient signal processing. The HHT estimates the instantaneous frequency (IF) using Hilbert transform (HT). However owing to the inevitable window effect of HT, the demodulation results present non-instantaneous response characteristic. An alternative approach developed by Maragos et al. [28-30] and Boudraa [32, 33] uses a nonlinear energy tracking operator, Teager Kaiser energy operator (TKEO), to first estimate the energy required for generating an AM-FM signal and then separate it into its instantaneous frequency (IF) and instantaneous amplitude (IA) components. Note that the Hilbert transform approach mainly involves a linear integral operator, whereas the TKEO approach uses a nonlinear differential operator. TKEO gives a good estimate of IF and has low computational complexity [30-33].

In this paper, we present a novel method to monitor bearing fault under run-up condition using order tracking, empirical mode decomposition (EMD) and nonlinear Teager Kaiser energy operator (TKEO), which is named as Teager-Huang transform (THT). This method is based on the re-sampling technique and Teager-Huang transform spectrum estimation of the re-sampled signal, which is a function of the angle of the input shaft of the gearbox. This re-sampling signal can be obtained by re-sampling of the vibration signal which has been previously sampled in the time domain. The Teager-Huang transform spectrum is based on the signal processing of the angle domain signal, where the resample signal is in accordance with the shaft angle of the gearbox. EMD is a fundamentally new approach to the decomposition of nonlinear and non-stationary signal presented originally by Huang [11]. EMD can decompose multi-components signal into a series of intrinsic mode functions (IMFs), then accurate instantaneous amplitude estimation can be acquired by TKEO. TKEO is a nonlinear operator that has been developed by Teager. It can track the energy and identify the instantaneous frequency and instantaneous amplitude of mono-component signal [28, 33]. In the end, time-frequency spectrum is obtained by using Teager-Huang transform. The characteristic frequencies related to the bearing defect can be effectively extracted. The basic method is introduced in detail. This approach is applied in the research of the fault detection and diagnosis of the roller bearing. The experimental results show that this method can effectively monitor the roller bearing faults.

To address the issues discussed above, this paper is organized as follows. Section 1 gives a brief introduction of the time-frequency analysis technology. Section 2 introduces the principles of computed order tracking. Section 3 gives a brief description of EMD and Hilbert-Huang transformation (HHT). Section 4 gives a brief introduction of Teager-Huang transform (THT). Section 5 presents the method and procedure of the bearing fault detection based on order tracking and THT. Section 6 gives two simulation examples to show the effectiveness and reliability of the proposed method. Section 7 describes the experimental set-up. Section 8 gives the application of the method based on order tracking and THT to fault detection and diagnosis of bearing. Section 9 gives the main conclusions of this paper.

2. The principles of computed order tracking

There are two popular techniques for producing synchronously sampled data: the traditional approach that uses special hardware to dynamically adapt the sample rate, and a tech-

nique where the vibration signals and a tachometer signal are synchronously sampled, that is, they are sampled conventionally at equal time increments. From the synchronously sampled tachometer signal re-sample times required to produce synchronous sampled data are calculated. This process is referred to as computed order tracking and is particularly attractive, as it requires no special hardware. Also, this approach is more flexible than the traditional method, as for example different sample rates may be synthesized. The computed order tracking is considerably more flexible than the traditional approach. It may be organized to produce equally accurate or more accurate results than the traditional method. An added benefit is that computed order tracking requires no specialized hardware, which is an important factor in many condition monitoring applications. Therefore, computed order tracking techniques are introduced and applied in this paper.

The objective of computed order tracking (COT) [21] is a calculation of the vibration signal sampled constant in angle from sampled constant in time. From the mathematical point of view, this task could be solved by interpolation theory.

The computed order tracking (COT) method first records the data at constant Δt increments, using conventional hardware, and then re-samples this signal to provide the desired constant $\Delta\theta$ data, based on a keyphasor signal.

To determine the resample times, it will be assumed that the shaft is undergoing constant angular acceleration. With this basis, the shaft angle $\theta(t)$ can be described by a quadratic equation of the following form [21]:

$$\theta(t) = b_0 + b_1 t + b_2 t^2 \tag{1}$$

The unknown coefficients b_0, b_1 and b_2 are found by fitting three successive keyphasor arrival times (t_1, t_2 and t_3), which occur at known shaft angle increments $\Delta\phi$. This can be obtained by the following conditions:

$$\begin{cases} \theta(t_1) = 0 \\ \theta(t_2) = \Delta\phi \\ \theta(t_3) = 2\Delta\phi \end{cases} \tag{2}$$

The arrival times t_1, t_2 and t_3 are known from the sampling of the keyphasor pulse signal.

Substituting these conditions into Eq. (1) and arranging in a matrix format gives,

$$\begin{pmatrix} 0 \\ \Delta\phi \\ 2\Delta\phi \end{pmatrix} = \begin{bmatrix} 1 & t_1 & t_1^2 \\ 1 & t_2 & t_2^2 \\ 1 & t_3 & t_3^2 \end{bmatrix} \begin{Bmatrix} b_0 \\ b_1 \\ b_2 \end{Bmatrix} \tag{3}$$

This set of equations is then solved for the unknown $\{b_i\}$ components. Once these values are known, Eq.1 may be solved for t, yielding

$$t = \frac{1}{2b_2}\left[\sqrt{4b_2(k\Delta\theta - b_0) + b_1^2} - b_1\right] \tag{4}$$

where k is the interpolation coefficient that can be obtained as follow:

$$\theta = k\Delta\theta \tag{5}$$

where θ is the shaft angle and $\Delta\theta$ is the desired angular spacing between resamples.

Once the resample times are calculated, the corresponding amplitudes of the signal are calculated by interpolating between the sampled data. After the amplitudes are determined, the re-sample data are transformed from the angle domain to the order domain by means of an FFT.

The order spectrum and Teager-Huang transform time-frequency spectrum are based on the signal processing of the angle domain signal, where the resample signal is in accordance with the shaft angle of the gearbox. The order spectrum and Teager-Huang transform time-frequency spectrum are then evaluated for the resample signal. The usefulness of this approach will be shown with an experimental example in Section 8.

3. Introduction of Hilbert-Huang transform (HHT)

Hilbert-Huang transformation is an emerging novel technique of signal decomposition having many interesting properties. To facilitate the reading of this paper we will introduce in detail the Hilbert-Huang transformation, which is a relatively novel technique.

3.1 The concept of intrinsic mode function

Huang et al. [11] have defined IMFs as a class of functions that satisfy two conditions:

1) In the whole data set, the number of extrema and the number of zero-crossings must be either equal or differ at most by one;

2) At any point, the mean value of the envelope defined by the local maxima and the envelope defined by the local minima is zero.

3.2 Empirical mode decomposition (EMD)

Empirical mode decomposition (EMD) has been proposed recently [11] as an adaptive time-frequency data analysis method. It has proven to be quite versatile in a broad range of applications for extracting signals from data generated in noisy nonlinear and non-stationary processes. As useful as EMD has proven to be, it still leaves some annoying difficulties unresolved.

Empirical mode decomposition method is developed from the simple assumption that any signal consists of different simple intrinsic mode oscillations. The essence of the method is to identify the intrinsic oscillatory modes (IMFs) by their characteristic times scales in the signal and then decompose the signal accordingly. The characteristics time scale is defined by the time lapse between the successive extremes.

To extract the IMF from a given data set, the sifting process

is implemented as follows. First, identify all the local extrema, and then connect all of the local maxima by a cubic spline line as the upper envelope. Then, repeat the procedure for the local minima to produce the lower envelope. The upper and lower envelopes should cover all the data between them. Their mean is designated $m_1(t)$, and the difference between the data and $m_1(t)$ is $h_1(t)$:

$$x(t) - m_1(t) = h_1(t) \tag{6}$$

Ideally, $h_1(t)$ should be an IMF, for the construction of $h_1(t)$ described above should have forced the result to satisfy all the definitions of an IMF by construction. To check if $h_1(t)$ is an IMF, we demand the following conditions: (i) $h_1(t)$ should be free of riding waves, i.e., the first component should not display under-shots or over-shots riding on the data and producing local extremes without zero crossing. (ii) To display symmetry of the upper and lower envelops with respect to zero. (iii) Obviously the number of zero crossing and extremes should be the same in both functions.

The sifting process has to be repeated as many times as it is required to reduce the extracted signal to an IMF. In the subsequent sifting process steps, $h_1(t)$ is treated as the data; then:

$$h_1(t) - m_{11}(t) = h_{11}(t) \tag{7}$$

where $m_{11}(t)$ is the mean of the upper and lower envelops of $h_1(t)$.

This process can be repeated up to k times; $h_{1k}(t)$ is then given by

$$h_{1(k-1)}(t) - m_{1k}(t) = h_{1k}(t) \tag{8}$$

After each processing step, checking must be done on whether the number of zero crossings equals the number of extrema.

The resulting time series is the first IMF, and then it is designated as $c_1(t) = h_{1k}(t)$. The first IMF component from the data contains the highest oscillation frequencies found in the original data $x(t)$.

This first IMF is subtracted from the original data, and this difference, is called a residue $r_1(t)$ by:

$$x(t) - c_1(t) = r_1(t) \tag{9}$$

The residue $r_1(t)$ is taken as if it was the original data and we apply to it again the sifting process. The process of finding more intrinsic modes $c_i(t)$ continues until the last mode is found. The final residue will be a constant or a monotonic function; in this last case it will be the general trend of the data.

$$x(t) = \sum_{j=1}^{n} c_j(t) + r_n(t) \tag{10}$$

Thus, one achieves a decomposition of the data into n-empirical IMF modes, plus a residue, $r_n(t)$, which can be either the mean trend or a constant.

3.3 The Hilbert-Huang transform (HHT)

Having obtained the IMFs using EMD method, one applies the Hilbert transform to each IMF component. With this definition $c_i(t)$ and $H[c_i(t)]$ form a complex conjugate pair, which defines an analytic signal $z_i(t)$:

$$z_i(t) = a_i(t)\exp(j\omega_i(t)) \tag{11}$$

with amplitude $a_i(t)$ and phase $\theta_i(t)$ defined by the expressions:

$$a_i(t) = \sqrt{c_i^2(t) + H^2[c_i(t)]} \tag{12}$$

$$\theta_i(t) = \arctan\left(\frac{H[c_i(t)]}{c_i(t)}\right) \tag{13}$$

Therefore the instantaneous frequency $\omega_i(t)$ can be given by:

$$\omega_i(t) = \frac{\mathrm{d}\theta_i(t)}{\mathrm{d}t} \tag{14}$$

Thus the original data can be expressed in the following form:

$$x(t) = \mathrm{Re}\sum_{i=1}^{n} a_i(t)\exp(j\int \omega_i(t)dt) \tag{15}$$

where the residue $r_n(t)$ has been left out. Re {.} denotes the real part of a complex quantity.

Eq. (15) enables us to represent the amplitude and the instantaneous frequency, in a three-dimensional plot, in which the amplitude is the height in the time-frequency plane. This time-frequency distribution is designated as the Hilbert-Huang spectrum $H(\omega,t)$:

$$H(\omega,t) = \mathrm{Re}\sum_{i=1}^{n} a_i(t)\exp(j\int \omega_i(t)dt) \tag{16}$$

4. Introduction of Teager-Huang transform (THT)

4.1 Teager kKaiser Energy operator (TKEO)

TKEO is a powerful nonlinear operator and has been successful used in many engineering application [32]. TKEO can track the modulation energy and identify the instantaneous frequency (IF) and the instantaneous amplitude (IA) of an amplitude modulation-frequency modulation (AM-FM) signal [29]. The TKEO, $\psi(.)$ is defined for continuous-time signal $x(t)$ as follows[32,33]:

$$\psi[x(t)] = [\dot{x}(t)]^2 - x(t)\ddot{x}(t) \tag{17}$$

where $\dot{x}(t)$ and $\ddot{x}(t)$ are the first and the second time derivatives of $x(t)$ respectively. In the discrete case, the time derivatives may be approximated by time differences. In discrete-time domain, TKEO is given as follows[28, 33]:

$$\psi[x(n)] = x^2(n) - x(n+1)\cdot x(n-1) \tag{18}$$

The instantaneous frequency $f(n)$ and instantaneous amplitude $|a(n)|$ at any time instant of the AM-FM signal $x(n)$ can respectinely be given as follows[28]:

$$y(n) = x(n) - x(n-1) \tag{19}$$

$$f(n) = ar\cos\left(1 - \frac{\psi[y(n)] + \psi[y(n+1)]}{4\psi[x(n)]}\right) \tag{20}$$

$$|a(n)| = \sqrt{\frac{\psi[x(n)]}{\sin^2[f(n)]}} \tag{21}$$

$$f(n) = \frac{1}{2}\arccos\left(1 - \frac{\psi[x(n+1) - x(n-1)]}{2\psi[x(n)]}\right) \tag{22}$$

$$|a(n)| = \frac{2\psi[x(n)]}{\sqrt{\psi[x(n+1) - x(n-1)]}} \tag{23}$$

In general, the demodulation method given by Eq. (19), Eq. (20) and Eq. (21) is named as discrete energy separation algorithm-1 (DESA-1). The demodulation method given by Eq. (22) and Eq. (23) is called as discrete energy separation algorithm-2 (DESA-2). In this paper, we calculate the instantaneous frequency $f(n)$ and instantaneous amplitude $|a(n)|$ by DESA-2. The DESA-2 algorithm only requires three samples for the energy computation at each time instant and is less computationally complex. Therefore, the DESA-2 algorithm has an excellent time resolution and almost instantanous. This excellent time resolution provides us with the ability to capture the energy fluctuations of the AM-FM signal.

4.2 The Teager-Huang transform (THT)

In order to estimate the instantaneous frequency $f(n)$ and instantaneous amplitude $|a(n)|$ of $x(t)$, the EMD is combined with the TKEO. TKEO can only be used to track the IF and IA of a monocomponent AM-FM signal. If $x(t)$ is a multi-component AM-FM signal, then bandpass filtering is needed to isolate each component before applying the discrete energy separation algorithm (DESA). Therefore, the EMD is used as a multiband filtering to separate the signal components in the time domain and hence reduce multi-component demodulation to multicomponent one. The conjunction of the EMD and the TKEO methods is called as Teager-Huang transform (THT) [33].

According to Eq. (22) and Eq. (23) the original data can be expressed in the following form:

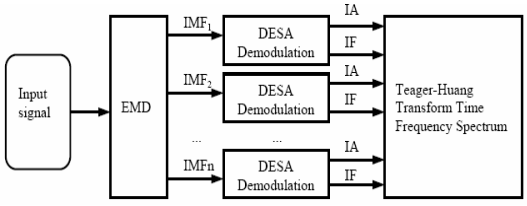

Fig. 1. Block diagram of the THT.

$$x(t) = \sum_{i=1}^{n} |a_i(t)| \exp(j\int 2\pi f_i(t)dt) \tag{24}$$

Eq. (24) enables us to represent the amplitude and the instantaneous frequency, in a three-dimensional plot, in which the amplitude is the height in the time-frequency plane. This time-frequency distribution is designated as the Teager-Huang spectrum $T(f,t)$:

$$T(f,t) = \sum_{i=1}^{n} |a_i(t)| \exp(j\int 2\pi f_i(t)dt) \tag{25}$$

The final presentation of the the IF and the IA results is an energy time frequency representation. The block diagram of Teager-Huang transform technique is illustrated in Fig.1. The original vibration signal can be decomposed into a series of monocomponent AM-FM signal named as IMFs. Then the IF and IA of the separated IMFs are calculated using the DESA-2 algorithm.

5. Proposed order tracking and THT method to fault detection of bearing

The procedure of proposed THT spectrum method is given as follows:

1) Non-stationary vibration signal under run-up condition is sampled using a constant time increment;

2) Non-stationary vibration signal is re-sampled at a constant angle increment. Then the non-stationary vibration signal in time domain is transformed into stationary one in angle domain;

3) To decompose the vibration signal $x(\theta)$ using EMD and to obtain IMFs;

4) To calculate the THT spectrum according to Section 4;

5) To draw a diagnostic conclusion according to the THT spectrum.

6. Signal simulation of THT spectrum

The performance of the proposed method has been assessed by means of tests on simulative signals. The multi-component signal, characterized by known instantaneous frequency trajectories, has been considered. The evolution versus time of the instantaneous frequency and amplitude of each component of the analyzed signal is finally showed.

A significant example is shown in Fig. 2. The signal shown

in Fig. 2 is composed of two components according to

$$x_1(t) = \cos[2\pi 40t + 0.5\sin(2\pi 20t)] \quad (26)$$

$$x_2(t) = \sin(2\pi 160t) \quad (27)$$

$$x(t) = x_1(t) + x_2(t) \quad (28)$$

Signal $x(t)$ is composed of a carrier frequency which is 40 Hz, frequency-modulated is 20 Hz and constant or time-independent frequency of 160 Hz sine wave.

Fig. 2 displays a graphical sketch of the signal $x(t)$, which was generated over a total time span T=0.2s with a sampling frequency $f_s = 2560$ Hz. Fig. 3 shows the empirical mode decomposition (EMD) in IMF of the signal $x(t)$. With the help of the sifting algorithm explained in Section 3, we carried out this decomposition. The decomposition identifies two modes: c_1 represents the sine wave of $x_2(t)$, c_2 represents the frequency modulated signal, $x_1(t)$, c_3 is the residue, respectively. By virtue of EMD method, a signal can be decomposed into two complete and orthogonal intrinsic mode functions. Therefore, we can know not only the frequency components of the signal, but also the variation of the amplitude and period. These IMFs component can reflect the actual physical meaning of the signal.

The THT spectrum of the simulative signal shown in Fig. 2 is displayed in Fig. 4 (contour plot) and Fig. 5 (mesh plot). Fig. 4 and Fig. 5 display the instantaneous frequency and the instantaneous amplitude estimation of multi-component signal $x(t)$ based on the ensemble empirical mode decomposition and TKEO. The IF in Fig.4 shows a clear picture of temporal frequency distribution of the data, i.e., the linear response has constant frequency at 160 Hz, the non-linear response has frequency dependence modulated around 40Hz and bounded by 30 and 50 Hz, and the decaying energy of the non-linear response with the color changing from the white at the beginning to dark blue at the end of the record. Therefore, the instantaneous frequency and the instantaneous amplitude estimation based on the ensemble empirical mode decomposition and TKEO are better to describe the characteristics of the time-frequency distribution.

To demonstrate the effectiveness of THT spectrum, let us compare how effective the Teager-Huang transform can be with the result from FFT, STFT, WVD, Morlet wavelet spectrum and HHT by considering the simulative signal shown in Fig. 2. The FFT of the simulative signal is given in Fig. 6. The Fourier spectrum should give the true frequency component, but it fails to give the true frequency distribution characteristics of frequency-modulated for $x_1(t)$. With STFT analysis we get the STFT spectrum in Fig. 7. In the result, neither the energy density nor the frequency distribution of frequency modulated for $x_1(t)$ is well localized. With Morlet wavelet analysis we get the spectrum in Fig.8, in which the characteristics of frequency-modulated for $x_1(t)$ are not well defined on the time frequency plane. In the result, neither the energy density nor the modulated frequency is well localized. Fig.9 shows the Wigner-Ville distribution of the signal $x(t)$, in which the cross terms are clearly evident as an oscillatory

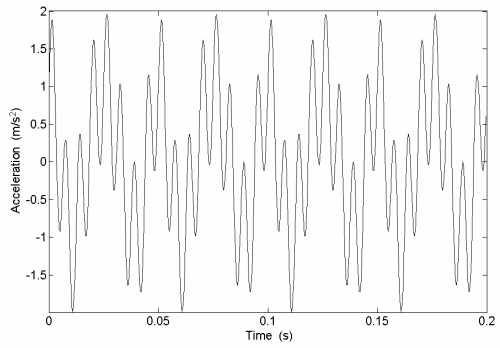

Fig. 2. Time domain signal of $x(t)$.

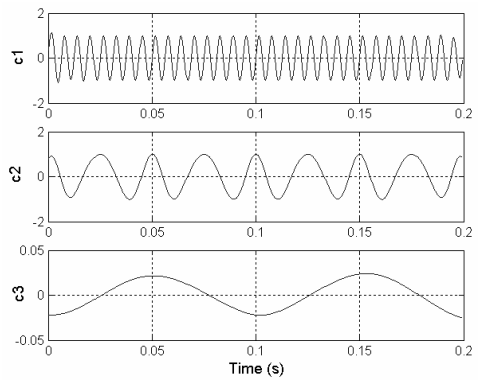

Fig. 3. The three IMFs component using EMD.

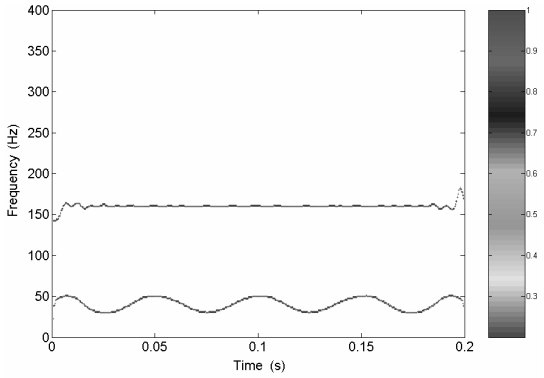

Fig. 4. THT spectrum of multi-components signal (contour plot).

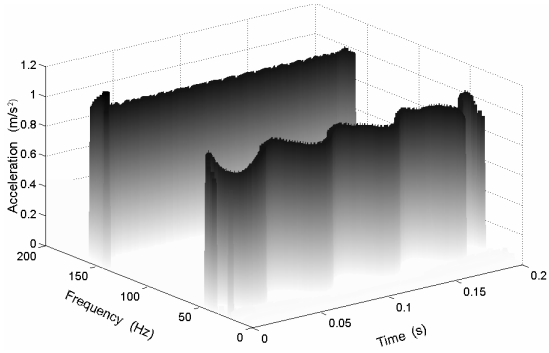

Fig. 5. THT spectrum of multi-components signal (mesh plot).

component midway between the two auto-terms. Moreover, the characteristic of frequency-modulating for $x_1(t)$ is not evident. When the same data are treated by the HHT spectral analysis, we have the result in Fig. 10, in which the energy is better localized in both frequency and time domains. However the frequency resolution of HHT is lower.

This simple simulation example illustrates the unique property of the THT spectrum in elimination of the spurious harmonic components to represent the non-stationary data and to analyze the multi-components vibration signal. Therefore, THT spectrum provides a viable signal-processing tool for machine fault detection and diagnosis.

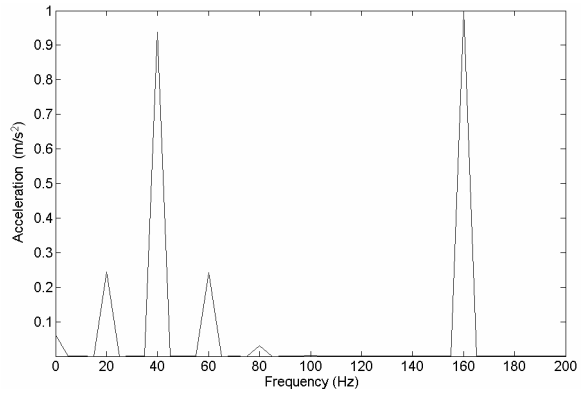

Fig. 6. FFT spectrum of multi-components signal.

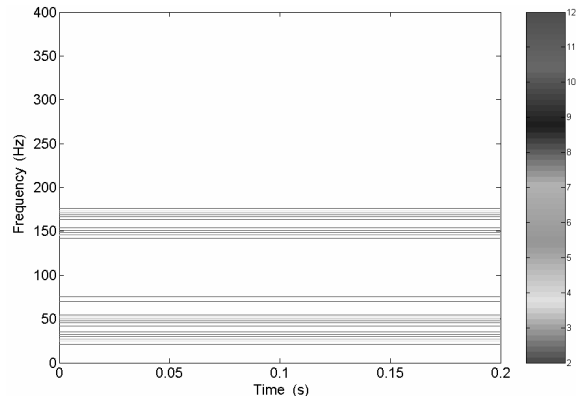

Fig. 7. STFT spectrum of multi-components signal.

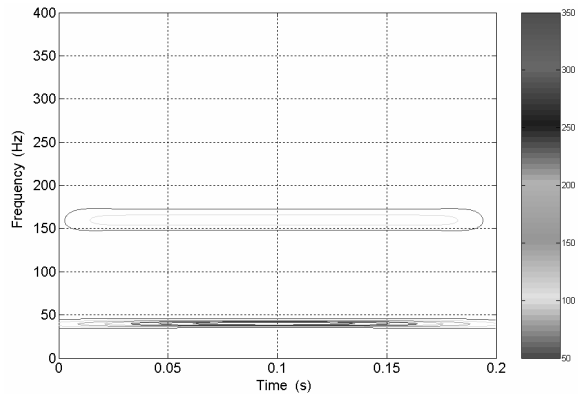

Fig. 8. Morlet wavelet time-frequency spectrum of multi-components signal.

7. Experimental set-up

The test apparatus used in this paper is shown in Fig. 11. The experimental set-up consists of a single-stage gearbox, driven by a 4.5 kW AC governor motor. The driving gear has 30 teeth and the driven gear has 50 teeth. Therefore, the transmission ratio is 50/30, which means that an decrease in rotation speed is achieved. The module of the gear is 2.5 mm. The monitoring and diagnostic system is composed of three accelerometers, amplifiers, a speed and torque transducer, B&K 3560 spectrum analyzer and a computer. The sampling span is 3.2 kHz, the sampling frequency is 8192 Hz, and the sampling time is 2 seconds. This time included one speed up of the gearbox from idle speed up to steady. After sampling, the measured vibration signals were loaded into MATLAB from data-files. Then, the vibration signals were re-sampled. For their re-sampling, the algorithm described in the previous section was used. As a result of experiment, the vibration signals generated by the tested gearbox were obtained sampled constant in time as well as sampled constant in angle.

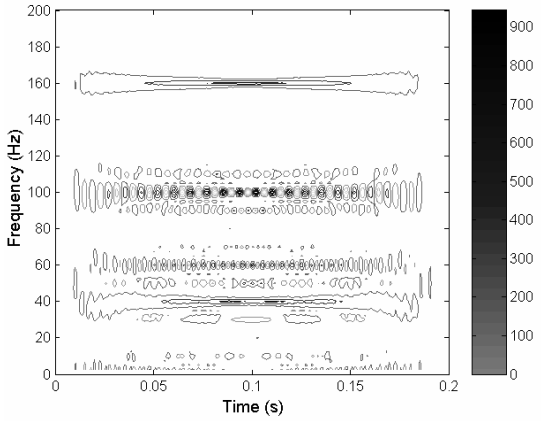

Fig. 9. Wigner-Ville distribution of multi-components signal.

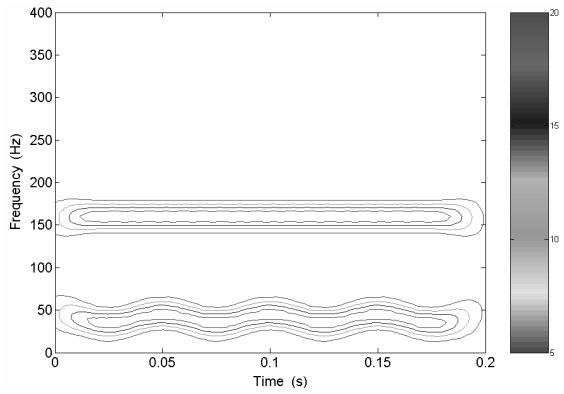

Fig. 10. HHT spectrum of multi-components signal.

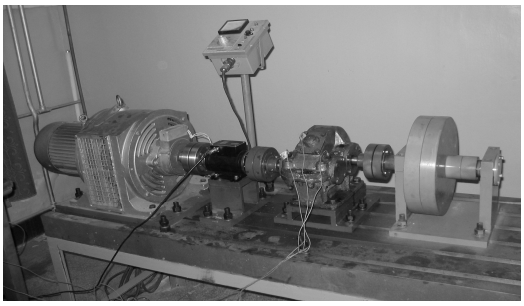

Fig. 11. Experimental set-up.

8. Bearing fault diagnosis based on order tracking and THT

In this section, the THT spectrum will be applied to vibration signal measured from a gearbox during speed up process.

Roller bearings are installed in many kinds of machinery. Many of the problems of those machines may be caused by ball bearing defects. Generally, localized defects may occur on inner race, outer race or rollers of bearing. A local fault may produce periodic impacts, the size and the repetition period which are determined by the shaft rotation speed, the type of fault and the geometry of the bearing. The successive impacts produce a series of impulse response, which maybe amplitude modulated because of the passage of fault through the load zone. The spectrum of such a signal would consist of a harmonics series of frequency components spaced at the component fault frequency with the highest amplitude around the resonance frequency. These frequency components are flanked by sidebands if there is an amplitude modulation due to the load zone. According to the period of the impulse, we can judge the location of the defect using characteristic frequency formulae. Because an inner race defect has more transfer segments when transmitting the impulse to the outer surface of the case, usually the impulse components are rather weak in the vibration signal.

The tested bearing was used to study only one kind of surface failure: the bearing was damaged on the race. The ball bearing tested had a groove on the inner race or outer race. Localized defect was seed on the race by an electric-discharge machine to keep their size and depth under control. The size of the artificial defect was 1mm in depth and the width of the groove was 1.5 mm. The type of the ball bearing is 206. There are 9 balls (z=9) in a bearing and the contact angle $\alpha = 0°$, ball diameter d=9.5mm, bearing pitch diameter D=41.75mm. Then the characteristic frequency of the inner race or outer race defect can be calculated according to Eq. (29) and Eq. (30), respectively.

$$f_{inner} = \frac{z}{2}\left(1 + \frac{d}{D}\cos\alpha\right) f_{r1} \tag{29}$$

$$f_{outer} = \frac{z}{2}\left(1 - \frac{d}{D}\cos\alpha\right) f_{r1} \tag{30}$$

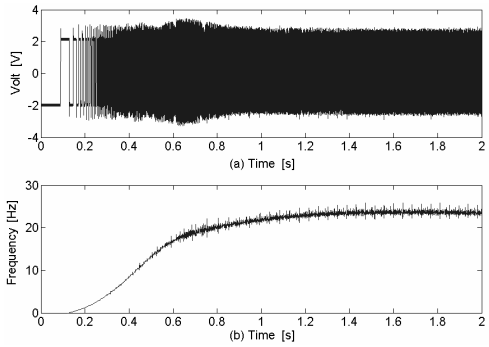

Fig. 12. Rotating speed of the input shaft.

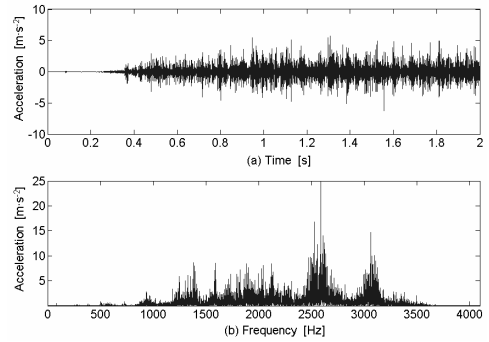

Fig. 13. Time-domain vibration signal with inner race fault and FFT.

where f_{r1} is the rotating frequency of the input shaft.

Therefore, according to Eq. (29) and Eq. (30), the characteristic frequency of the inner race and outer race defect is given as follows:

$$f_{inner} = 5.42 f_{r1} \tag{31}$$

$$f_{outer} = 3.58 f_{r1} \tag{32}$$

Then the characteristic order of the inner race and outer race is obtained:

$$O_{inner} = 5.42 \tag{33}$$

$$O_{outer} = 3.58 \tag{34}$$

8.1 Application of order tracking and THT to fault detection of inner race

The rotating speed signal of the input shaft for the tested gearbox is displayed in Fig. 12. Fig. 12(a) represents the sampling pluses of the input shaft from the optical encoder (60 pulses per rotational period). The encoder signals consist of 16384 points and have a total duration of 2 seconds. To obtain approximate values of rotational speed for every data point, polynomial curve fitting was used. It was found that linear approximate was sufficient for this research. Polynomial coefficients were determined for each data, and analytical descriptions of the rotational speed were obtained. Fig. 12(b) is the calculated instantaneous rotating speed using interpolating

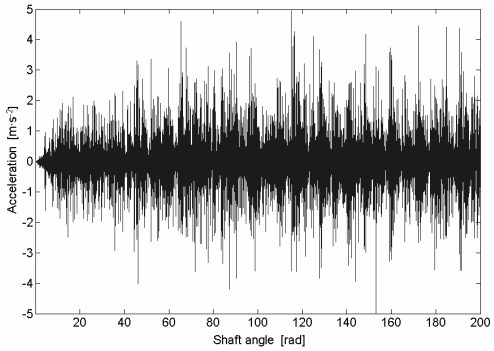

Fig. 14. Angular resample signal of Fig. 13(a).

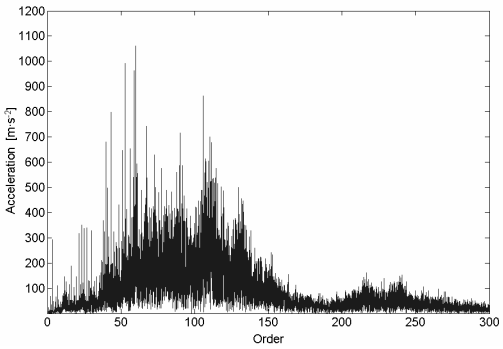

Fig. 15. Order spectrum of inner race fault.

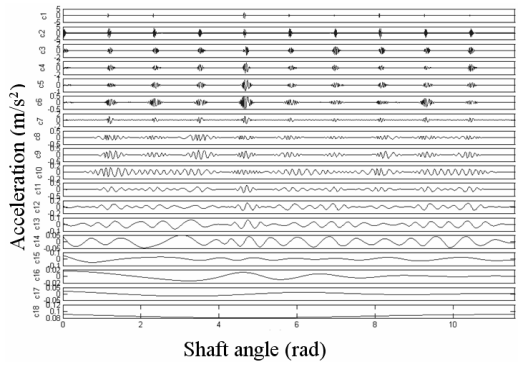

Fig. 16. IMFs of the resample signal shown in Fig. 14.

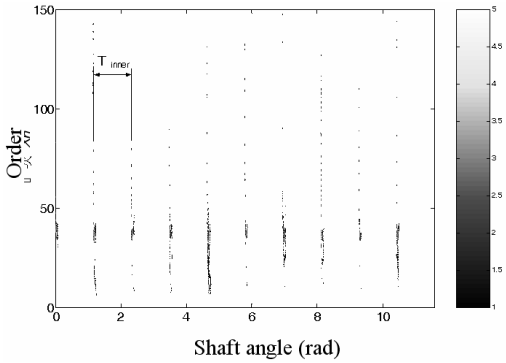

Fig. 17. THT spectrum of vibration signal shown in Fig. 15.

method. Fig. 12(b) clearly shows that the rotating speed of the input shaft runs up from idle to steady speed about 700 rpm.

The original vibration signal with inner race fault is displayed in Fig. 13(a). Fig. 13(a) shows that the vibration signals are non-stationary, of which the amplitude of the vibration is increasing while the input shaft speeds up. The result of applying conventional spectral analysis (FFT) to the specified non-stationary signal is given in Fig. 13(b). Fig. 13(b) displays the FFT of the vibration signals with inner race fault. It is clear that the resulting spectrum is significantly obscured by spectral smearing. Besides, traditional spectral averaging cannot be applied to the non-stationary signal during the input shaft run up. Fig. 13(b) clearly shows that spectral smearing substantially affects the result of conventional analysis based on time sampling. Therefore, classical Fourier analysis has some limitation such as being unable to process non-stationary signals.

The angular re-sample method is applied to the vibration signal of Fig. 13(a). Fig. 14 displays the re-sample vibration signal with uniform angular increment of 0.008722 rad. It is clear that there are periodic impacts in the angle domain vibration signal. There are significant fluctuations in the peak amplitude of the signal. However it is hardly possible to evaluate the bearing fault condition only through such angle domain vibration signal. Fig. 15 shows a high resolution order power spectrum of the re-sample vibration signal. The order power spectrum, as shown in Fig. 15, is dominated by the repetition order of the gear mesh order and its harmonics. It can be seen from Fig. 15, that the order power spectrum represents the complicated quantities. This complexity of the order power spectrum follows from the frequency smearing and modulation effects. Therefore, the conventional order power spectrum was not capable of revealing the characteristic order of inner race fault that was corrupted by the modulation and noise.

To the resample data of Fig. 14, the EMD algorithm is applied. Fig. 16 displays the empirical mode decomposition in eighteen IMFs of the resample vibration signal in Fig. 14. The decomposition identifies eighteen modes: c_1 - c_{17} represents the frequency components excited by the inner race defects, and c_{18} is the residue, respectively. Mode c_1 contains the highest signal frequencies, mode c_2 the next higher frequency band and so on.

From Fig. 16, it can be easily proven that the EMD decomposes the resample vibration signal very effectively on an adaptive method. The Teager-Huang transform can be applied to each IMF $c_i(t)$, resulting in THT spectrum according to Eq. (25). The corresponding results of the THT analysis are illustrated in Fig.17. The presence of inner race fault results in a sudden increase of vibration energy. For the defective bearing, transient vibrations caused by the rollers-defect interactions are clearly seen in frequency range of 10-150 orders. In addition, these transient vibrations have shown a repetitive pattern with a T_{inner} =1.1587rad ($T_{inner} = 2\pi/\hat{x}_{inner}$) interval, which corresponds to a repetitive the characteristic cycle of the inner race, resulting from the structural defect on the inner race. Such a repetitive cycle reflects degradation of the inner race health condition as the defect propagated through the bearing inner race. Physically, impacts generated by the roll-

ing ball-defect interactions excite intrinsic modes of the bearing system, giving rise to a train of transient vibrations at the mode-related resonant frequencies. The simplicity of the order quantity representation can be put down to the ability of the order signal processing method to eliminate undesirable spectral smearing and modulation effects. Therefore, the THT has shown to provide an effective tool for bearing inner fault diagnosis.

8.2 Application of order tracking and THT to fault detection of outer race

Fig. 18(a) shows the original vibration signal with outer race fault while the input shaft speeds up. Fig. 18(b) displays the FFT of the vibration signal with outer race fault. It is clear that the resulting spectrum is the same as the inner race fault that is significantly obscured by spectral smearing.

Fig. 19 displays the re-sample vibration signal with uniform angular increment. Fig. 20 is the order power spectrum of the re-sample vibration signal. The conventional order power spectrum was not capable of revealing the characteristic order of outer race fault in the same way.

To the resample data of Fig. 19, the EMD algorithm is applied. Fig. 21 displays the empirical mode decomposition in eighteen IMFs of the resample vibration signal in Fig.19.The decomposition identifies eighteen modes: c_1 - c_{17} represents the frequency components excited by the outer race defects, and c_{18} is the residue, respectively. Mode c_1 contains the highest signal frequencies, mode c_2 the next higher frequency band and so on.

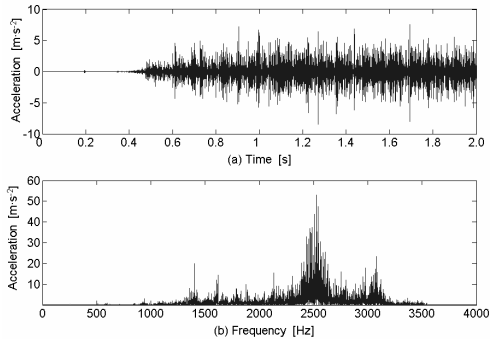

Fig. 18. Time-domain vibration signal with outer race fault and FFT.

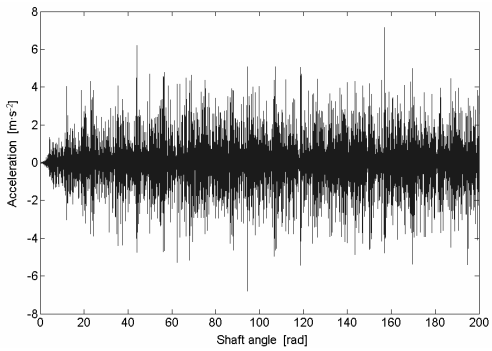

Fig. 19. Angular resample signal of Fig. 18(a).

The Teager-Huang transform can be applied to each IMF $c_i(t)$, resulting in THT spectrum according to Eq. (25). The corresponding results of the THT analysis are illustrated in Fig.22. The presence of outer race fault results in a sudden increase of vibration energy. For the defective bearing, transient vibrations caused by the rollers-defect interactions are clearly seen in frequency range of 7-150 orders. In addition, these transient vibrations have shown a repetitive pattern with a T_{outer} =1.7542rad ($T_{outer} = 2\pi / \hat{x}_{outer}$) interval, which corresponds to a repetitive characteristic cycle of the outer race, resulting from the structural defect on the outer race. Such repetitive cycle reflects degradation of the outer race health condition as the defect propagated through the bearing outer race. Physically, impacts generated by the rolling ball-defect interactions excite intrinsic modes of the bearing system, giving rise to a train of transient vibrations at the mode-related resonant frequencies. The simplicity of the order quantity

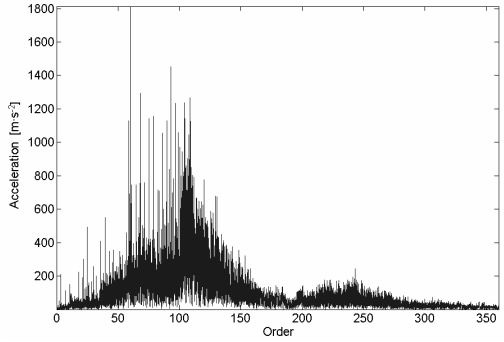

Fig. 20. Order spectrum of outer race fault.

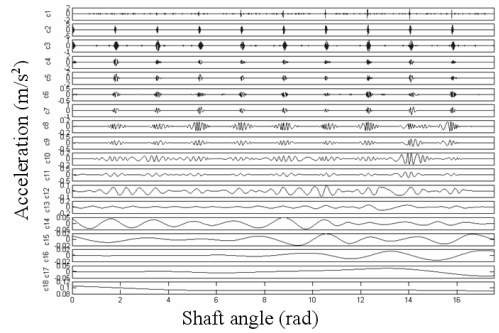

Fig. 21. IMFs of the resample signal shown in Fig. 19.

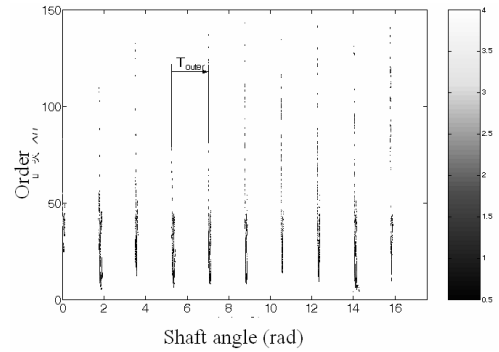

Fig. 22. THT spectrum of resample signal shown in Fig. 19.

representation can be put down to the ability of the order signal processing method to eliminate undesirable spectral smearing and modulation effects. Therefore, the THT has shown to provide an effective tool for bearing outer fault diagnosis.

9. Conclusions

A method for fault diagnosis of rolling bearing was presented based on a newly developed signal processing technique named as computed order tracking, empirical mode decomposition (EMD) and Teager Kaiser energy operator (TKEO). Using computed order-tracking, the non-stationary vibration signals during run-up of bearing faults in time domain can be transformed into stationary one in the angle domain. Using EMD method, the resample vibration signals of bearing faults can be decomposed into intrinsic modes. Therefore, we can recognize the vibration modes that coexist in the system, and have a better understanding of the nature of the fault information contained in the vibration signal. According to the Teager-Huang transform spectrum, the characteristic period of the bearing faults can be easily recognized. Practical vibration signal monitored from a gearbox during running up with bearing fault is analyzed by the presented method. The experimental result has shown that the Teager-Huang transform can be used as an effective diagnostic method for bearing faults. Such a technique can be further applied to the health detection of other of dynamic systems, such as electrical drives. Research is being continued to systematically investigate the suitability and constraints of the THT for non-stationary signal analysis, using vibration signals from different types of bearings.

Acknowledgments

The authors are grateful to the National Natural Science Foundation of China (No.50775219 and No.50975185), Zhejiang Provincial Natural Science Foundation (No.Y 1080040). The authors are also grateful to the editors and reviewers for their constructive comments.

References

[1] L. Cohen, *Time-frequency analysis* , Prentice-Hall, Englewood Cliffs, NJ, 1995.

[2] J. Lin and L. Qu, Feature extraction based on Morlet wavelet and its application for mechanical fault diagnosis, *Journal of Sound and Vibration,* 234 (1) (2000) 135-148.

[3] W. J. Staszewski, Wavelet based compression and feature selection for vibration analysis*, Journal of Sound and Vibration,* 211 (5) (2000) 736-760.

[4] C. James Li and Jun Ma, Wavelet decomposition of vibration for detection of bearing-localized defects, *NDT&E International,* 30 (3) (1997) 143-149.

[5] S. Prabhakar, A. R.Mohanty and A. S. Sekhar, Application of discrete wavelet transform for detection of ball bearing race fault*, Tribology International,* 3 (12) (2002) 793-800.

[6] W. J. Wang and P. D. Mcfadden, Application of orthogonal wavelet to early gear damage detection, *Mechanical Systems and Signal Processing,* 9 (5) (1995) 497-507.

[7] W. J. Staszewski, K. Worden and G. R. Tomlinson, Thefrequency analysis in gearbox fault detection using the Wigner-Ville distribution and pattern recognition*, Mechanical Systems and Signal Processing,* 11 (5) (1997) 673-692.

[8] L. Galleani and L. Cohen, The Wigner distribution for classical system, *Physics Letters A,* 302 (4) (2002) 149-155.

[9] G. Matz and F. Hlawatsch, Wigner distribution (nearly) everywhere: time-frequency analysis of signals, systems, random process, signal spaces, and frames*, Signal Processing,* 83 (7) (2003) 1355-1378.

[10] F. Hlawatsch and W. Kozek, The Wigner distribution of a linear signal space*, IEEE transaction on signal processing,* 41 (3) (1993) 1248-1258.

[11] N. E Huang, Z. Shen and S. R. Long et al, The empirical mode decomposition and the Hilbert spectrum for nonlinear and non-stationary time series analysis*, Proceeding of Royal Society London, Series A,* 454 (1998) 903-995.

[12] H. Li, Y. Zhang and H. Zheng, Wear Detection in Gear System Using Hilbert-Huang Transform, *Journal of Mechanical Science and Technology*, 20 (11) (2006) 1781-1789.

[13] E. Lopatinskaia, J. Zhu and J. Mathew, Monitoring varying speed machinery vibration — I. The use of non-stationary recursive filters, *Mechanical Systems and Signal Processing*, 9 (6) (1995) 635-645.

[14] E. Lopatinskaia, J. Zhu and J. Mathew, Monitoring varying speed machinery vibration —II. Recursive filters and angle domain, *Mechanical Systems and Signal Processing*, 9 (6) (1995) 647-655.

[15] G. Meltzer and Y. Y.Ivanov, Fault detection in gear drives with non-stationary rotational speed—part I: the time-frequency approach, *Mechanical Systems and Signal Processing*, 17 (5) (2003) 1033-1047.

[16] G. Meltzer and Y. Y.Ivanov, Fault detection in gear drives with non-stationary rotational speed—part II: the time-quefrency approach, *Mechanical Systems and Signal Processing*, 17 (2) (2003) 273-283.

[17] JianDa Wu, ChinWei Huang and Rongwen Huang, An application of a recursive kalman filtering algorithm in rotating machinery fault diagnosis, *NDT&E International*, 37 (3) (2004) 411-419.

[18] Zhinong Li, Zhaotong Wu, Yongyong He and Chu Fulei, Hidden Markov model-based fault diagnostics method in speed-up and speed-down process for rotating machinery, *Mechanical Systems and Signal Processing*, 19 (2) (2005) 329-339.

[19] R. Potter, A New Order Tracking Method for Rotating Machinery, *Sound and Vibration*, 7 (1990) 30-34.

[20] R. Potter and M. Gribler, Computed Order Tracking Obsoletes Older Methods, *Proceedings of the SAE Noise and Vibration conference*, (1989) 63-67.

[21] K. R. Fyfe and E. D. S.Munck, Analysis of computed order tracking, *Mechanical Systems and Signal Processing*, 11 (2) (1997) 187-205.

[22] K. M. Bossley and R. J. Mckendrick, Hybrid computed order tracking, *Mechanical Systems and Signal Processing*, 13 (4) (1999) 627-641.

[23] N. E. Huang, Z. Shen and S. R. Long, A new view of nonlinear water waves: The Hilbert spectrum*, Annual Review of Fluid Mechanics,* 31 (1999) 417-457.

[24] J. Nunes, Y. Bouaoune, E. Delechelle, O. Niang and P. Bunel, Image analysis by bidimensional empirical mode decomposition*, Image and Vision Computing,* 21 (2003) 1019-1026.

[25] S. Quek, P. Tua and Q. Wang, Detecting anomalies in beams and plate based on the Hilbert-Huang transform of real signals*, Smart Materials and Structures,* 12 (2003) 447-460.

[26] S. J. Loutridis, Damage detection in gear system using empirical mode decomposition *Engineering Structure,* 26 (2004) 1833-1841.

[27] H. Li, H. Zheng and L. Tang, Wigner-Ville Distribution Based on EMD for Faults Diagnosis of Bearing, *Lecture Notes in Computer Science*, 4223 (2006) 803-812.

[28] P. Maragos, J. F. Kaiser and T. F. Quatieri, Energy separation in signal modulations with application to speech analysis, *IEEE Transactions on Signal Processing*, 41 (10) (1993) 3024- 3051.

[29] P. Maragos, J. F. Kaiser and T. F. Quatieri, On amplitude and frequency demodulation using energy operators. *IEEE Transactions on Signal Processing*, 41 (5) (1993) 1532-1550.

[30] D. Vakman, On the analytic signal, the Teager-Kaiser energy algorithm, and other methods for defining amplitude and frequency, *IEEE Transactions on Signal Processing*, 44 (4) (1996) 791- 797.

[31] A. Potamianos and P. Maragos, A comparison of the energy operator and the Hilbert transform approach to signal and speech demodulation, *Signal Processing,* 37 (1) (1994) 95-120.

[32] J. C. Cexus and A. O. Boudraa, Teager-Huang analysis applied to sonar target recognition, *International Journal of Signal Processing*, 1 (1) (2004) 23-27.

[33] J. C. Cexus and A. O. Boudraa, Nonstationary signals analysis by Teager-Huang Transform (THT), *Proceedings of EUSIPCO*, (2006) 1-5.

Hui Li received his B.S. in Mechanical Engineering from the Hebei Polytechnic University, Hebei, China, in 1991. He received his M.S. in Mechanical Engineering from the Harbin University of Science and Technology, Heilongjiang, China, in 1994. He received his Ph.D from the School of Mechanical Engineering of Tianjin University, Tianjin, China, in 2003. He was a postdoctoral researcher in Shijiazhuang Mechanical Engineering College from August 2003 to September 2005, and in Beijing Jiaotong University from March 2006 to December 2008. He is currently a professor in Mechanical Engineering at Shijiazhuang Institute of Railway Technology, China. His research and teaching interests include hybrid driven mechanism, kinematics and dynamics of machinery, mechatronics, CAD/CAPP, signal processing for machine health monitoring, diagnosis and prognosis. He is currently a senior member of the Chinese Society of Mechanical Engineering.